Blockade of cardiac sarcoplasmic reticulum K^+ channel by Ca^{2+}: two-binding-site model of blockade

Qi-Yi Liu and Harold C. Strauss
Departments of Pharmacology and Medicine, Duke University Medical Center, Durham, North Carolina 27710 USA

ABSTRACT Potassium countercurrent through the SR K^+ channel plays an important role in Ca^{2+} release from the SR. To see if Ca^{2+} regulates the channel, we incorporated canine cardiac SR K^+ channel into lipid bilayers. Calcium ions present in either the SR lumenal (*trans*) or cytoplasmic (*cis*) side blocked the cardiac SR K^+ channel in a voltage-dependent manner. When Ca^{2+} was present on both sides, however, the block appeared to be voltage independent. A two-binding site model of blockade by an impermeant divalent cation (Ca^{2+}) can explain this apparent contradiction. Estimates of SR Ca^{2+} concentration suggest that under physiological conditions the cardiac SR K^+ channel is partially blocked by Ca^{2+} ions present in the lumen of the SR. The reduction in lumenal [Ca^{2+}] during Ca^{2+} release could increase K^+ conductance.

INTRODUCTION

Muscle contraction is initiated by the rapid release of Ca^{2+} through the sarcoplasmic reticulum Ca^{2+} release channel (1, 2). The Ca^{2+} release channels of both skeletal and cardiac SR have been intensively investigated (3–5). If the SR membrane were permeable only to Ca^{2+}, its membrane potential would very rapidly approach the Ca^{2+} equilibrium potential, and Ca^{2+} release would dramatically decrease (6, 7). Some countermovement of other ions could minimize the potential change and help compensate for the large Ca^{2+} flux. Studies of skeletal and cardiac SR membrane permeability demonstrated that mammalian skeletal and cardiac SR vesicles contain ion-conducting pathways allowing for K^+, Na^+, H^+ and Cl^- flux (8, 9). There is compelling evidence to indicate that K^+ flux in skeletal SR vesicles occurs via the SR K^+ channel (8, 10–12) and represents an important countercurrent for Ca^{2+} release (13). The SR K^+ channels from cardiac and skeletal muscle share many properties, although there are appreciable differences in gating and conduction (14,15). The dramatic change in calcium concentrations in the cardiac SR lumen and cytoplasm during muscle contraction (16, 17) may affect the conductance of the cardiac SR K^+ channel. Knowledge of these effects would advance our understanding of the physiologic role of Ca^{2+} in the SR and cytoplasm.

METHODS

Cardiac SR vesicles were prepared from canine ventricular tissue as described previously (15, 18). The vesicles were used immediately or stored at −80°C. Phospholipid bilayers were formed with phosphatidylethanolamine (PE; Avanti Polar Lipids, Incorporated, Birmingham, AL) in decane (20 mg/ml) across a 0.3-mm hole separating a 50 or 150 mM K-acetate, 10 mM histidine, pH 7.2 solution. Vesicles were added to the *cis* chamber. We incorporated the SR K^+ channel into the lipid bilayer and then perfused the chambers with the desired solutions. We held the *trans* chamber at virtual ground and monitored current across the bilayer via a high input impedance electrometer configured in the current-to-voltage mode. The current signal was digitized and stored on VCR tape for further analysis, low pass filtered at 100 Hz (8-pole Bessel), displayed on an oscilloscope, and recorded on a chart recorder as described previously (15, 18). We used macroscopic Ca^{2+} ion-selective electrodes (TIPCA; World Precision Instruments, Incorporated, New Haven, CT) to measure Ca^{2+} activity in a parallel series of experiments. All Ca^{2+} measurements are expressed as activities.

Address correspondence to Dr. Harold C. Strauss.

RESULTS AND DISCUSSION

We incorporated cardiac SR K^+ channels into planar lipid bilayers and observed that over 90% of the channels were oriented in the same direction as reported for the skeletal muscle SR K^+ channel (12, 19). Miller et al. (12) proposed that the side of the channel facing the *cis* chamber corresponds to the cytoplasmic side of the channel. This was confirmed by the similarities in the open probability-voltage relationship between patch clamp studies of lobster remotor muscle SR K^+ channel (20) and the reconstituted SR K^+ channel (12, 14, 18, 21).

In the absence of Ca^{2+}, the conductance of the fully open state was 131 ± 5.1 ps at 50 mM KAc (n = 12) and 153.8 ± 6.2 pS at 150 mM KAc (n = 10). When Ca^{2+} was added symmetrically to the bathing solutions (*cis* and *trans* chambers) between 0.1–30 mM Ca^{2+}, the K^+ current of the fully open state (O_2) and the main substate (O_1) underwent a Ca^{2+} concentration-depen-

0006-3495/91/07/198/06 $2.00

dent reduction without detectable flickering (Fig. 1 *A*). However, a detailed analysis of the effects of Ca^{2+} was performed only on the fully open state current. We describe the reduction of the K^+ current by a simple blockade scheme,

$$\text{open} + Ca^{2+} \underset{k_{-1}}{\overset{k_1}{\leftrightarrow}} \text{blocked},$$

where Ca^{2+} is impermeant, and once it binds to the channel, K^+ cannot pass through. The blocking and unblocking rates k_1 and k_{-1} appear to be rapid relative to the recorder's bandwidth, so the current amplitude is a weighted average of the open and blocked state currents. In symmetrical 50 mM K^+ solution with Ca^{2+} activity from 0 to 15 mM, the current-voltage relationship was nearly linear from −60 mV to +60 mV (Fig. 1 *B*)).

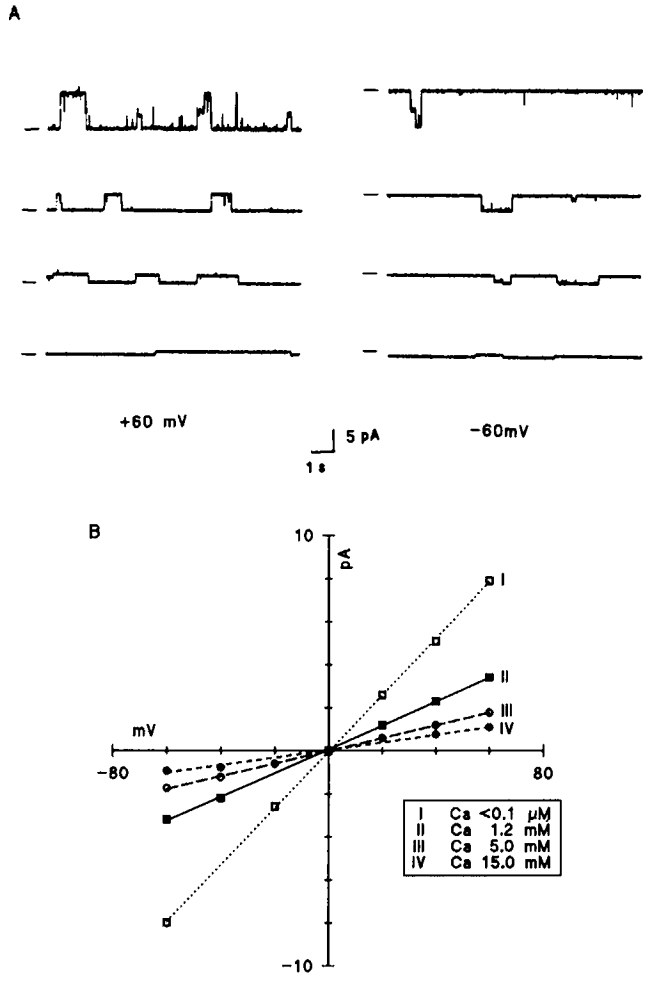

FIGURE 1 K^+ current blockade by symmetric Ca^{2+}. (*A*) Single-channel current recordings from canine cardiac SR K^+ channel incorporated into a planar lipid bilayer. Single-channel currents, shown as upward (V > 0) or downward (V < 0) deflections, were recorded in symmetric 50 mM KAc, 10 mM histidine, pH 7.1 with Ca^{2+} activity < 0.1 μM (top trace), $[Ca^{2+}]$ = 1.2 mM (second trace), $[Ca^{2+}]$ = 5 mM (third trace) and $[Ca^{2+}]$ = 30 mM (bottom trace) in both *cis* and *trans* chambers. (*B*) I-V relationship for the fully open state (O_2) at different Ca^{2+} activities in a neutral bilayer (PE only). Similar results were seen in four other experiments.

When Ca^{2+} was added to only one side of the channel, we saw a pronounced voltage-dependent current reduction. Current-voltage relationships at several different *cis* (*A*) and *trans* (*B*) Ca^{2+} activities for a typical experiment are illustrated in Fig. 2 *A* and *B*. We used neutral lipid (PE) to form the bilayers to minimize possible screening effects of Ca^{2+} ions. Reduction of the K^+ current was concentration dependent, regardless of the side to which Ca^{2+} was added, although Ca^{2+} block from the *trans* side was slightly more effective. To determine whether Ca^{2+} could contribute to the current, K^+ was replaced in one of the chambers by 50 or 90 mM Ca^{2+}. No Ca^{2+} current was observed in four experiments either from *cis* to *trans* (*cis* side perfusion, Fig. 3) or from *trans* to *cis* (*trans* side perfusion, data not shown). Furthermore, the reversal potential did not shift when we increased Ca^{2+} activity to high levels, in the absence of Tris, on one side of the membrane (in 15 experiments), also indicating that the channel does not conduct Ca^{2+}. The apparent reversal potential under biionic conditions suggested a permeability ratio of a $P_K/P_{Ca} >$ 100, which is consistent with the findings of a recent patch clamp study of the skeletal SR K^+ channel (22).

Because Ca^{2+} can block the channel from either side without passing through it, the simplest interpretation is that there are two independent binding sites within the channel that are accessible to Ca^{2+}. We propose a revision of Woodhull's model (23, 24), with two binding sites separated by a high central barrier that prevents Ca^{2+} permeation. Further, Ca^{2+} can bind only to the site on the side where it entered the channel (Fig. 3 *A*, *inset*). Once Ca^{2+} binds to a site, the channel is blocked. With Ca^{2+} present in one side, we can describe the blockade by the following equations:

$$\frac{\gamma}{\gamma_o} = \left\{1 + \frac{[Ca^{2+}]_c}{K(0)_c} e^{z\delta_c FV/RT}\right\}^{-1}, \text{ for } \textit{cis}\ Ca^{2+}, \quad (1)$$

$$\frac{\gamma}{\gamma_o} = \left\{1 + \frac{[Ca^{2+}]_t}{K(0)_t} e^{z\delta_t FV/RT}\right\}^{-1}, \text{ for } \textit{trans}\ Ca^{2+}, \quad (2)$$

where γ and γ_o are conductances in the presence and absence of Ca^{2+}; $[Ca^{2+}]_c$ and $[Ca^{2+}]_t$ are Ca^{2+} activity in *cis* and *trans* chambers; $K(0)_c$ and $K(0)_t$ are the apparent zero-voltage dissociation constants of Ca^{2+}; δ_c and δ_t are the fractional electrical distances of the *cis* and *trans* binding sites; z is the valence of the blocker; V is the holding potential; and F, R, and T have their usual meanings. As shown in Fig. 4 *A* and *B*, the consistently

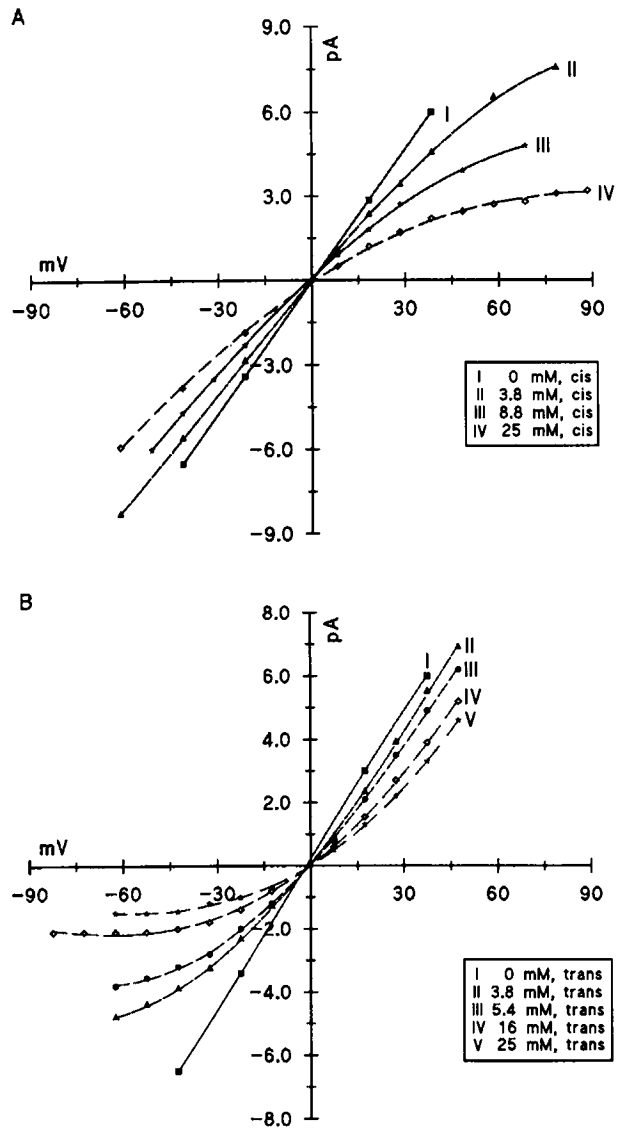

FIGURE 2 K^+ current blockade by asymmetric Ca^{2+}. (*A* and *B*) I-V relationships for the fully open state at different Ca^{2+} ion activities. A smooth curve with cubic spline fit to the data points has no attached significance. K^+ current is blocked by Ca^{2+} present on either *cis* (*A*) or *trans* (*B*) side of the bilayer. Experimental conditions in the two experiments were symmetric 150 mM KAc, 1.2 mM Mg^{2+}, 10 mM histidine, pH 7.2 solution with neutral bilayer (PE only). Similar results were obtained in four other experiments.

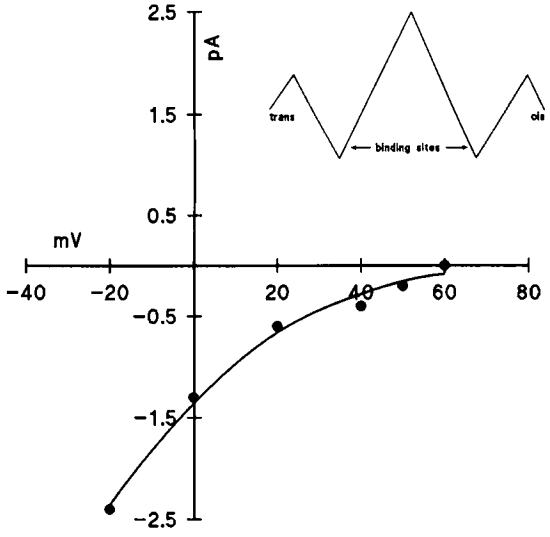

FIGURE 3 Impermeability of Ca^{2+}. After SR K^+ channel was incorporated into the bilayer at 150 mM KAc bathing solution, the *cis* chamber was perfused by 90 mM $CaCl_2$, 250 mM HEPES/Tris, pH 7.2 solution. A typical experiment illustrates that no current fluctuation could be resolved for V > 60 mV. A free energy profile of the cardiac SR K^+ channel for Ca^{2+} is shown in the inset.

linear relationship between $ln\ (\gamma_o/\gamma - 1)$ and the holding potential strongly support the mechanism of blockade as described by Eqs. 1 and 2. In 150 mM K^+ solution, for *cis* block $K(0)_c = 21 \pm 2.3$ mM, and $\delta_c = 0.18 \pm 0.01$ ($n = 5$); for *trans* block $K(0)_t = 15.2 \pm 2.0$ mM and $\delta_t = -0.24 \pm 0.02$ ($n = 6$). The different values of δ_c and δ_t indicate that our data cannot be accounted for by a model with only one binding site. Ca^{2+} binding is competitive with K^+ (at 100 mM $[K^+]$, $K(0)_c = 14$ mM and $K(0)_t = 10$ mM). On the other hand, δ_c and δ_t are independent of K^+ and Ca^{2+} concentration (data not shown), suggesting that the configuration of the channel protein remains stable with varying K^+ and Ca^{2+} concentration.

When Ca^{2+} is present on both sides of the bilayer, it can bind to either site. Hence, K^+ conductance will be proportional to the probability that neither of the two sites are occupied by Ca^{2+}, given by the product of the probabilities of *cis* and *trans* sites being unoccupied. According to our model, the probabilities that the *cis* and *trans* sites being unoccupied will be proportional to $\{1 + [Ca^{2+}]_c/K(0)_c \exp(-z\delta_c FV/RT)\}^{-1}$ and $\{1 + [Ca^{2+}]_t/K(0)_t \exp(-z\delta_t FV/RT)\}^{-1}$, respectively. Thus, K^+ conductance reduces to:

$$\frac{\gamma}{\gamma_o} = \left\{1 + \frac{[Ca^{2+}]_c}{K(0)_c} e^{z\delta_c FV/RT} + \frac{[Ca^{2+}]_t}{K(0)_t} e^{z\delta_t FV/RT} + \frac{[Ca^{2+}]_c[Ca^{2+}]_t}{K(0)_c K(0)_t} e^{z(\delta_c+\delta_t)FV/RT}\right\}^{-1} \quad (3)$$

The curves shown in Fig. 4 *C* were generated according to Eq. 3 with $K(0)_c$, $K(0)_t$, δ_c, and δ_t obtained from experiments in which Ca^{2+} was added to only one side. A simple calculation using Eq. 3 indicates that γ will be nearly independent of holding potential over a large voltage range (Fig. 4 *D*). As the driving force increases, the nonlinear current–voltage relation becomes detect-

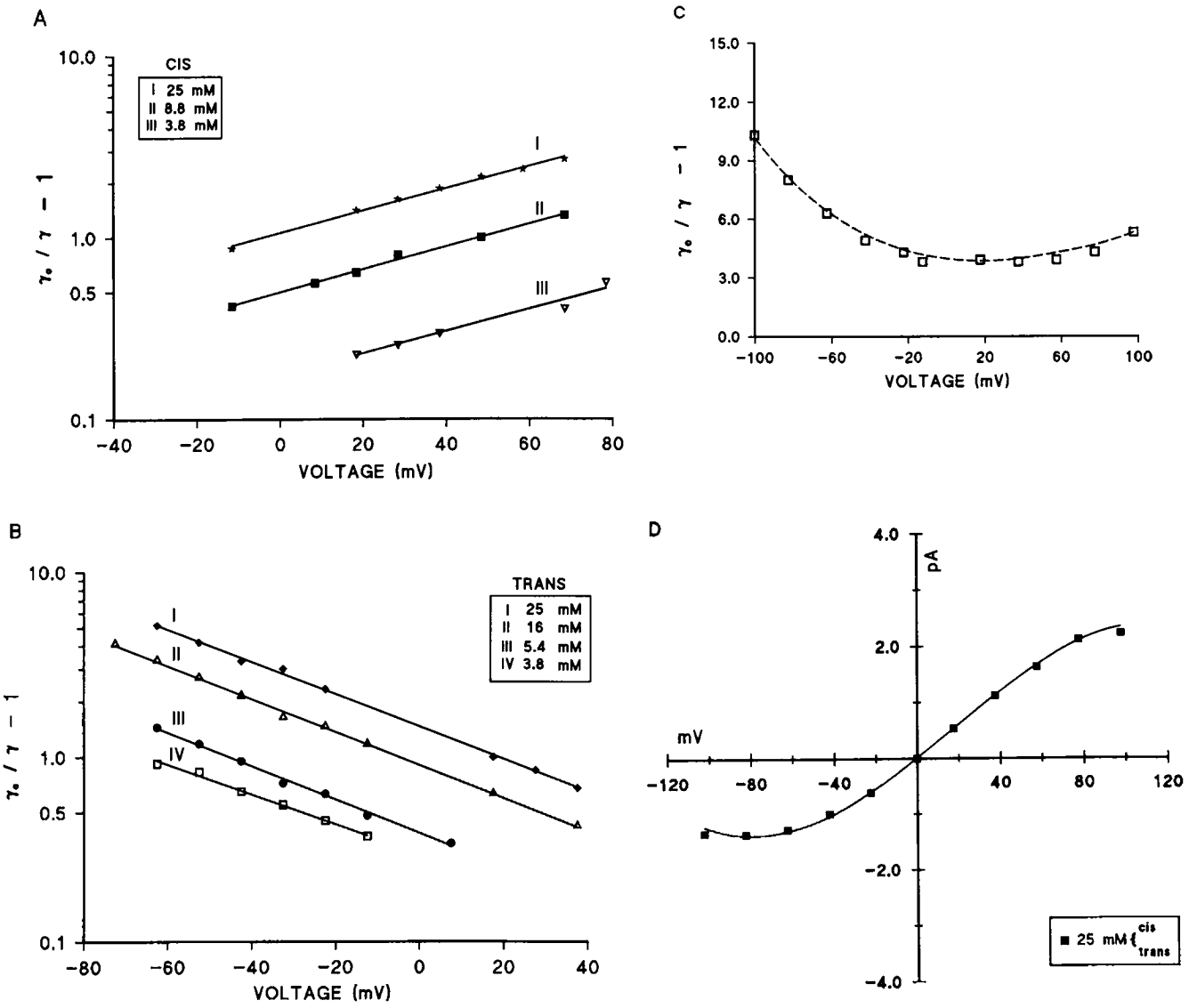

FIGURE 4 Two-binding-site model of blockade. (*A* and *B*) Voltage dependence of asymmetric Ca^{2+} block. Chord conductances were determined from the experiments shown in Fig. 2. Linear regression lines were fit to the data points obtained at different *cis* (*A*) and *trans* (*B*) Ca^{2+} activities in 150 mM KAc, 1.2 mM Mg^{2+}, 10 mM histidine, pH 7.2 solution with neutral bilayer (PE only). Mean values of $K(0)_c = 21$ mM, $\delta_c = 0.18$, $K(0)_t = 15$ mM, $\delta_t = -0.23$ were computed from data derived at different calcium levels. (*C*) Voltage dependence of symmetric Ca^{2+} block. Experimental data for symmetric 150 mM KAc, 1.2 mM Mg^{2+}, 10 mM histidine, 25 mM symmetrical Ca^{2+} activity, pH 7.2 solution with neutral bilayer. The curve superimposed on the data points is the theoretical prediction according to Eq. 3 for the following values, $K(0)_c = 23$ mM, $K(0)_t = 17$ mM, $\delta_c = 0.17$, and $\delta_t = -0.22$. (*D*) Current–voltage relationships are shown for the experiments under the same conditions as *C*. Theoretical curve superimposed on the data points used the values of the parameters indicated in the description of *C*.

able (Fig. 4*D*). The voltage range over which the conductance decrease is voltage-independent will depend on the K^+ and Ca^{2+} concentrations.

Although the cardiac and skeletal muscle SR K^+ channels are functionally similar, important differences have been noted. For example, Cs^+ and bis-quaternary ammonium block both the skeletal (11–12, 25–28) and cardiac (14, 15) SR K^+ channels. While the affinities of blockers from the *cis* or *trans* sides of the cardiac SR K^+ channel are similar, the affinities of blockers from the two sides of the skeletal muscle SR K^+ channel differ by several orders of magnitude. Similarly, Ca^{2+} blocked the skeletal SR K^+ channel from the *cis* side only (10). Further, the fractional electrical distance of the Cs^+ binding site from the *cis* side is ~0.20 for the cardiac SR K^+ channel (15) and ~0.38 for the skeletal muscle SR

K^+ channel (26). Models of decamethonium block in skeletal SR K^+ channel assume a single binding site (12, 28), whereas the fractional electrical distances estimated for *cis* and *trans* block of decamethonium in the cardiac SR K^+ channel indicate that two binding sites exist (14). Determination of the exact location of the binding sites within the pore is complicated by the uncertainty of the configuration of the compound, which led to the consideration of another possible binding site (14). Calcium blockade is easier to analyze as it is a point-charge particle, and our data indicate that there are two Ca^{2+} binding sites in the cardiac SR K^+ channel.

Recent data indicate that in the appropriate K^+ concentration range the cardiac SR K^+ channel behaves as a multi-ion pore (15). However, Hill et al. calculated that the probability of two K^+ ions occupying the channel simultaneously is less than ~ 0.01 in the K^+ concentration range we used (15). We have found that Ca^{2+} block is voltage dependent, that the fractional electrical distance (<1) is independent of K^+ and Ca^{2+} concentration in the range we studied, and that Ca^{2+} block is competitive with K^+ concentration. These results are consistent with the channel behaving as a single-ion channel, and, thus, in the K^+ and Ca^{2+} concentration ranges studied, our model represents a reasonable approximation of the permeation process. Several impermeant channel blockers appear to bind to two sites in the cardiac (14) and skeletal (29) SR K^+ channels and, as a result, our model may be useful in probing the structure of these and other channels with two binding sites.

Current estimates of resting Ca^{2+} concentration in the SR lumen under physiological conditions range between 0.5 and 5.0 mM (6, 30, 31). Accordingly, at rest the cardiac SR K^+ channel could be partially blocked by Ca^{2+} ions present in the lumen of the SR (corresponding to the *trans* side for the reconstituted channel). Electron probe microanalysis studies indicate that cardiac SR Ca^{2+} is decreased by 42% at peak contraction relative to control (17). This fall in SR $[Ca^{2+}]$ could reduce Ca^{2+} block of the channel and could increase K^+ conductance. Because Ca^{2+} blockade of the skeletal SR K^+ channel occurs only from the *cis* side (10), the change in SR $[Ca^{2+}]$ during Ca^{2+} release could not affect its conductance. Since cytoplasmic (*cis*) free Ca^{2+} concentration only increases from nanomolar to micromolar range during contraction, this change in cytosolic Ca^{2+} has little effect on conductance for either the cardiac or the skeletal SR K^+ channel.

We are indebted to Drs. J. Ma, D. L. Campbell, and G. Meissner for reading an earlier version of the manuscript. We are also indebted to S. Webb and A. Crews for their assistance in the preparation of this manuscript.

This work was supported by grants HL-19216 and 45132 from the Heart, Lung, and Blood Institute of the National Institutes of Health.

Received for publication 5 November 1990 and in final form 4 February 1991.

REFERENCES

1. Endo, M. 1977. Calcium release from sarcoplasmic reticulum. *Physiol. Rev.* 57:71–108.
2. Fabiato, A. 1983. Calcium-induced release of Ca^{2+} from the cardiac sarcoplasmic reticulum. *Am. J. Physiol.* 245:C1–C14.
3. Lai, F. A., H. P. Erickson, E. Rousseau, Q-Y. Liu, and G. Meissner. 1988. Purification and reconstitution of the calcium release channel from skeletal muscle. *Nature (Lond.).* 331:315–319.
4. Takeshima, H., S. Nishimura, T. Matsumoto, H. Ishida, K. Kangawa, N. Minamino, H. Matsuo, M. Ueda, M. Hanocka, T. Hirose, and S. Numa. 1989. Primary structure and expression from complementary DNA of skeletal muscle ryanodine receptor. *Nature (Lond.).* 339:439–445.
5. Anderson, K., F. A. Lai, Q-Y. Liu, E. Rousseau, H. P. Erickson, and G. Meissner. 1989. Structural and functional characterization of the purified cardiac ryanodine receptor Ca^{2+} release channel complex. *J. Biol. Chem.* 264:1329–1335.
6. Oetliker, H. 1982. An appraisal of the evidence for a sarcoplasmic reticulum membrane potential and its relation to calcium release in skeletal muscle. *J. Muscle Res. Cell. Motil.* 3:247–272.
7. Baylor, S. M., W. K. Chandler, and M. W. Marshall. 1984. Calcium release and sarcoplasmic reticulum membrane potential in frog skeletal muscle fibers. *J. Physiol.* 348:209–238.
8. Meissner, G. 1983. Monovalent ion and calcium ion fluxes in sarcoplasmic reticulum. *Mol. Cell. Biochem.* 55:65–82.
9. Meissner, G., and D. McKinley. 1982. Permeability of canine cardiac sarcoplasmic reticulum vesicles to K^+, Na^+, H^+, and Cl^-. *J. Biol. Chem.* 257:7704–7111.
10. Miller, C. 1978. Voltage-gated cation conductance channel from fragmented sarcoplasmic reticulum. *J. Membr. Biol.* 40:1–23.
11. Coronado, R., R. L. Rosenberg, and C. Miller. 1980. Ionic selectivity, saturation and block in a K^+-selective channel from sarcoplasmic reticulum. *J. Gen. Physiol.* 76:425–446.
12. Miller, C., J. E. Bell, and M. Garcia. 1984. The potassium channel of sarcoplasmic reticulum. *Curr. Top. Membr. Transp.* 21:99–132.
13. Abramcheck, C. W., and P. M. Best. 1989. Physiological role and selectivity of the in situ potassium channel of the sarcoplasmic reticulum in skinned frog skeletal muscle fibers. *J. Gen. Physiol.* 93:1–21.
14. Tomlins, B., A. J. Williams, and R. A. P. Montgomery. 1984. The characterization of a monovalent cation-selective channel of mammalian cardiac muscle sarcoplasmic reticulum. *J. Membr. Biol.* 80:191–199.
15. Hill, J. A. Jr., R. Coronado, and H. C. Strauss. 1989. Potassium channel of cardiac sarcoplasmic reticulum is a multi-ion channel. *Biophys. J.* 55:35–46.
16. Wier, W. G. 1990. Cytoplasmic $[Ca^{2+}]$ in mammalian ventricle dynamic control by cellular processes. *Annu. Rev. Physiol.* 52:467–485.
17. Moravec, C. S., and M. Bond. 1990. X-ray microanalysis of

subcellular calcium distribution in contracted and relaxed cardiac muscle. *Biophys. J.* 57:503a. (Abstr.)

18. Hill, J. A. Jr., R. Coronado, and H. C. Strauss. 1990. Open channel subconductance state of the K^+ channel from cardiac sarcoplasmic reticulum. *Am. J. Physiol.* 258:H159–H164.
19. Miller, C., and R. L. Rosenberg. 1979. A voltage-gated cation conductance channel from fragmented sarcoplasmic reticulum. Effect of transition metal ions. *Biochemistry.* 18:1138–1145.
20. Tang, J. M., J. Wang, and R. S. Eisenberg. 1989. K^+-selective channel from sarcoplasmic reticulum of split lobster muscle fibers. *J. Gen. Physiol.* 94:261–278.
21. Labarca, P., R. Coronado, and C. Miller. 1980. Thermodynamic and kinetic studies of the gating behavior of a K^+-selective channel from the sarcoplasmic reticulum membrane. *J. Gen. Physiol.* 76:397–424.
22. Stein, P. G., T. E. Nelson, and P. T. Palade. 1989. Mammalian sarcoplasmic reticulum K channels recorded in skinned fibers. *Biophys. J.* 55:480a. (Abstr.)
23. Woodhull, A. M. 1973. Ionic blockade of sodium channels in nerve. *J. Gen. Physiol.* 61:687–708.
24. Hille, B. 1984. Ionic Channels of Excitable Membranes. Sinauer Associates, Inc., Sunderland, MA. 277–279.
25. Coronado, R., and C. Miller. 1979. Voltage-dependent caesium blockade of a cation channel from fragmented sarcoplasmic reticulum. *Nature (Lond.).* 280:807–810.
26. Cukierman, S., G. Yellen, and C. Miller. 1985. The K^+ channel of sarcoplasmic reticulum. A new look at Cs^+ block. *Biophys. J.* 48:477–484.
27. Coronado, R., and C. Miller. 1980. Decamethonium and hexamethonium block of K^+ channel of sarcoplasmic reticulum. *Nature (Lond.).* 288:495–497.
28. Miller, C. 1982. Bis-quaternary ammonium blockers as structural probes of the sarcoplasmic reticulum K^+ channel. *J. Gen. Physiol.* 79:869–891.
29. Oosawa, Y., and M. Sokabe. 1986. Voltage-dependent aminoglycoside blockade of the sarcoplasmic reticulum K^+ channel. *Am. J. Physiol.* 250:C361–C364.
30. Hasselbach, W., and H. Oetliker. 1983. Energetics and electrophysiology of the sarcoplasmic reticulum calcium pump. *Annu. Rev. Physiol.* 45:325–339.
31. Meissner, G. 1984. Adenine nucleotide stimulation of Ca^{2+}-induced Ca^{2+} release in sarcoplasmic reticulum. *J. Biol. Chem.* 259:2365–2374.